Journal of Magnetics 13(2), 37-42 (2008)

< Invited Review Paper>

Optimized Design of Low Voltage High Current Ferrite Planar Inductor for 10 MHz On-chip Power Module

Seok Bae[1,2], Yang-Ki Hong[1,2]*, Jae-jin Lee[1,2], Gavin Abo[1,2], Jeevan Jalli[1,2], Andrew Lyle[1,2], Hongmei Han[1,2], and Gregory W. Donohoe[3]

[1]*Department of Electrical and Computer Engineering, University of Alabama, Tuscaloosa, AL 35487, USA*
[2]*MINT Center, University of Alabama, Tuscaloosa, AL 35487, USA*
[3]*Department of Electrical and Computer Engineering, University of Idaho, Moscow, ID 83844, USA*

(Received 15 May 2008)

In this paper, design parameters of high Q (> 50), high current inductor for on-chip power module were optimized by 4 *X*s 3 *Y*s DOE (Design of Experiment). Coil spacing, coil thickness, ferrite thickness, and permeability were assigned to *X*s, and inductance (L) and Q factor at 10 MHz, and resonance frequency (f_r) were determined *Y*s. Effects of each *X* on the *Y*s were demonstrated and explained using known inductor theory. Multiple response optimizations were accomplished by three derived regression equations on the *Y*s. As a result, L of 125 nH, Q factor of 197.5, and f_r of 316.3 MHz were obtained with coil space of 127 μm, Cu thickness of 67.8 μm, ferrite thickness of 130.3 μm, and permeability 156.5. Loss *tan* δ = 0 was assumed for the estimation. Accordingly, Q factor of about 60 is expected at *tan* δ = 0.02.

Keywords : DC-DC converter, DOE, ferrite inductor, Ni-Zn-Cu ferrite, on-chip power module, optimization

1. Introduction

The input voltage of the base-band processor is lowered to avoid overheat of finer conduction line [1], which is the same trend for other CPUs. Consequently, current needs to increase up to several amperes in a smart phone as shown in Fig. 1. In order to achieve small ripple voltage, the integrated and miniaturized on-chip power module has been intensively studied. On the other hand, an increase in switching frequency decreases inductance (L) and capacitance (C) in the power circuit resulting in size reduction and integration of passive components. The switching frequency of a commercial DC-DC converter has already been increased up to 5 MHz [2] and higher frequency [3, 4]. A high Q inductor is an essential component for high efficiency DC-DC converters. Therefore, a DC-DC converter with an air-core chip inductor was proposed [4, 5] to achieve high Q at high frequency. However, the air-core inductor Q is still below 20 in the 10~100 MHz range.

In this work, we proposed the 1~2 W buck-type one-chip power module having 0.25 V and 5 A output as shown in Fig. 2. And then, the optimized design parameters of a ferrite planar inductor, which has high Q over 50 at 10~100 MHz, for use in the one-chip power module were reported. We used DOE (Design of Experiment; one of the common six-sigma tools) method to optimize space and thickness of copper coil and thickness and perme-

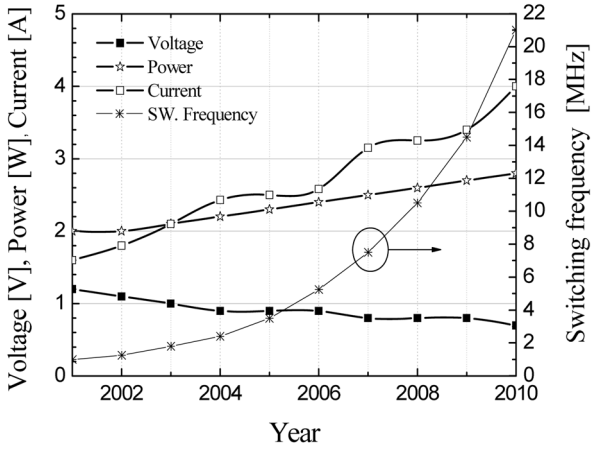

Fig. 1. Voltage, current, power, and switching frequency in a single dc-dc converter [1].

*Corresponding author: Tel: +1-205-348-7268
Fax: +1-205-348-6959, e-mail: ykhong@eng.ua.edu

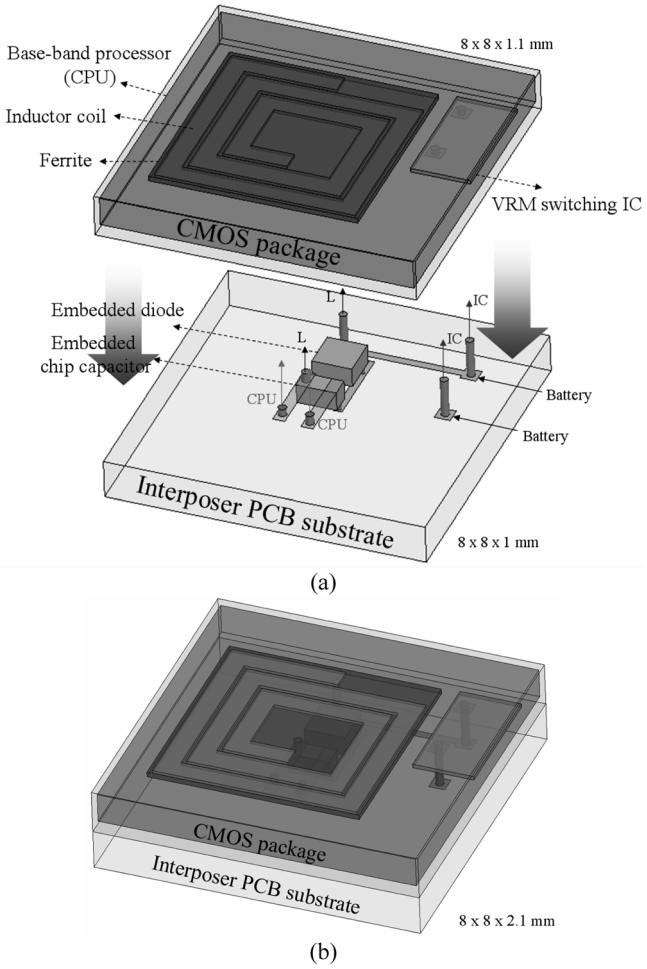

Fig. 2. Proposed one-chip power module; (a) CMOS package and interposer PCB substrate, and (b) assembled module.

ability of the ferrite film.

2. Design Parameters and DOE

2.1. Design parameters

2.1.1. Structure

A UA-C type spiral inductor design is used because of its high L/area property [6]. The UA-C type spiral inductor is described in Fig. 3. Copper coil with area of 5×5 mm^2 was designed on a 600 μm thick Si substrate. Copper coil thickness is in the range of 50-100 μm and is assigned as an *X* factor of the DOE. These thicknesses are greater than double the skin depth at 10 MHz. Cross-sectional coil area was designed 0.025 mm^2 to withstand joule heating by maximum 5 A rated current. This value is determined from references of high current inductors [7, 8]. Therefore, line width of Cu coil is fixed at 500 μm. Coil spacing is assigned as an *X* factor of the DOE and is in the range of 2~500 μm. In principal, inductor needs

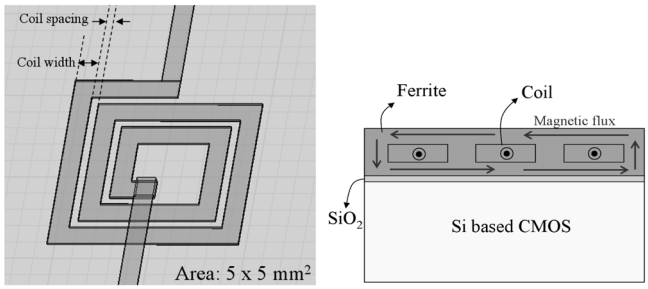

Fig. 3. Inductor structure of UA-C spiral 2.5 turns inductor; (a) plain view and (b) cross sectional view on the left lines of the coil.

inductance of 125 nH at 10 MHz. These are calculated by Wong's critical inductance equation [9]. Accordingly, 2.5 turns of spiral coil was determined.

2.1.2. Magnetic material

Ferrite inductor shows better performances than magnetic metal alloy inductor because of its excellent parasitic properties [6]. Therefore, Ni-Zn-Cu ferrite was selected for the magnetic material of the inductor. According to Nakamura [10], average μ_r of 200 is achievable at 10 MHz. Permeability is assigned as an *X* factor of the DOE and is in the range of 2~1000. Ferrite crystallization below 400 °C, the allowable temperature of integration process on Si substrate, is possible by Pulse laser deposition (PLD) [11], sputtering [12], aero-sol deposition (AD) [13], ferrite plating [14], and electrophoretic deposition (EPD) [15]. PLD and sputtering are thin film processes. The other AD (2.8 μm/min), ferrite plating (0.23 μm/min), and EPD (0.4 μm/min) are suitable to fabricate thick film. Finally, ferrite thickness is assigned as an *X* factor of the DOE and is in the range of 2~500 μm.

2.2. Design of Experiment

2.2.1. DOE

In order to optimize the design parameters, a 4 *X*s 3 *Y*s 3 level DOE is carried out. The 25 *X*-*Y* conditions were determined by $2 \times n + 2^n + 1$ (n = number of Xs) as a central composite design of DOE. The *Y*s of 25 inductors with different *X*s were simulated and analyzed. The DOE-Pro software, commercial package, is used for this analysis. The fixed parameters, 4 *X*s, and 3 *Y*s are shown in Table 1. L and Q factor at 10 MHz and f_r of inductor are chosen as the 3 *Y*s, which are the most important performance factors of the inductor. According to the results of multiple regression analysis, three regression equations on the *Y*s are derived using a completed design sheet of 25

Table 1. 4 Xs, 3 Ys and fixed parameters.

4 Xs	Fixed parameters	3 Ys
Coil spacing Cu thickness Ferrite thickness Permeability	UA-C Spiral design Coil material = Cu Mag. Material = Ni-Zn-Cu ferrite; tan δ = 0 Coil area = 5×5 mm^2 Coil turns = 2.5 turns Coil width = 500 μm	L at 10 MHz Q at 10 MHz Resonance frequency

inductors. A multiple response optimization is accomplished using these equations. The targets of optimization are L = 125 nH at 10 MHz and weight 50%, Q factor > 100 and weight 40%, and f_r > 200 MHz and weight 10%. The f_r is weighted lower than others, because f_r values are over 100 MHz in almost all of the simulated inductors.

2.2.2. Simulation

Ansoft HFSS software based on 3D FEM simulation was used for modeling of the inductor and calculation of S-parameters. S-parameters were converted into Y-parameters by equations (1), (2), and (3). The equivalent circuit parameters of L_s, Q, R_s, R_1, R_2, C_{21}, C_{22}, etc. were calculated by equations (4), (5), (6), (7), and (8) from the equivalent circuit theory of magnetic film inductor [16].

$$Y_{11}=\frac{(1-s_{11})(1+s_{22})+s_{12}s_{21}}{(1+s_{11})(1+s_{22})-s_{12}s_{21}} \tag{1}$$

$$Y_{12}=\frac{-2s_{12}}{(1+s_{11})(1+s_{22})-s_{12}s_{21}} \tag{2}$$

$$Y_{22}=\frac{(1+s_{11})(1-s_{22})+s_{12}s_{21}}{(1+s_{11})(1+s_{22})-s_{12}s_{21}} \tag{3}$$

$$-Y_{12}\frac{1}{R_s+J\omega L_s} \tag{4}$$

$$Y_{11}+Y_{12}=\frac{1}{R_1}+J\omega C_{21} \tag{5}$$

$$Y_{22}+Y_{12}=\frac{1}{R_2}+J\omega C_{22} \tag{6}$$

$$L_s=\frac{1}{2\pi f}img\left(\frac{1}{Y_{11}}\right) \tag{7}$$

$$R_s=real\left(\frac{1}{Y_{11}}\right) \tag{8}$$

$$Q=\frac{\mathrm{Im}(1/Y_{11})}{\mathrm{Re}(1/Y_{11})} \tag{9}$$

Where; L_s: inductance of spiral coil, R_s: resistance of spiral coil, Q: quality factor of spiral coil, C_{21}: capacitance between spiral coil and ground plane, R_1: parallel resistance with C_{21}, C_{22}: capacitance at the inner port of spiral coil, R_2: parallel resistance with C_{22}.

3. Results and Disscusion

The effective weights of the 4 *X*s (space, Cu thickness, ferrite thickness, permeability) on the 3 *Y*s are evaluated and demonstrated in Fig. 4. L of the inductor is the most dependent on the permeability (μ) and ferrite thickness while Q factor is dependent on the ferrite and Cu thickness. Coil spacing and ferrite terms of permeability and ferrite thickness evenly affect the f_r.

L is significantly increased with μ as shown in Fig. 5(c) and (d). The increasing ratio of L/μ is getting larger as well, as ferrite thickness increases. The effect of coil di-

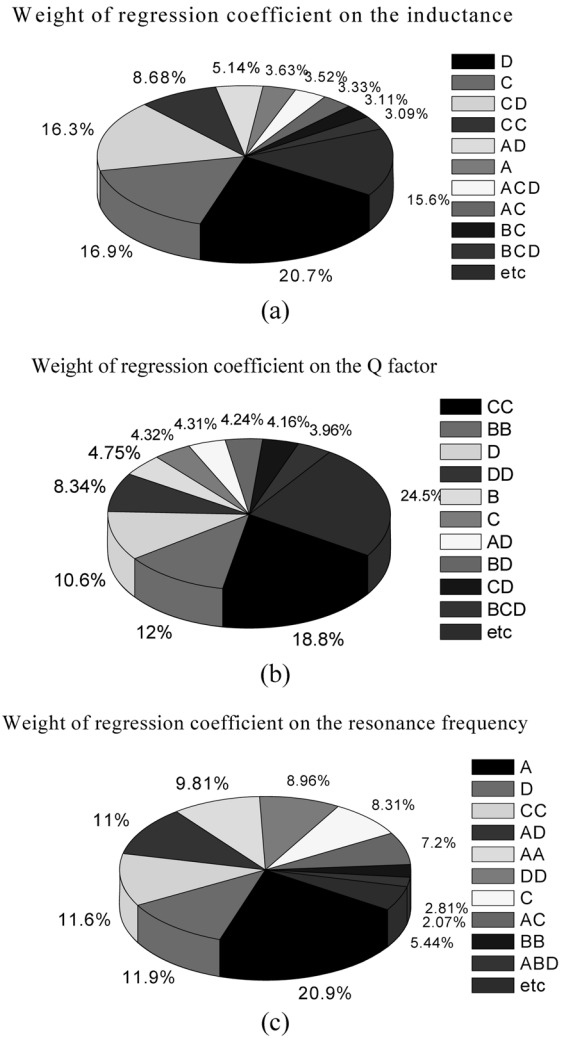

Fig. 4. Pie charts about weight of *X*'s for *Y*'s (L, Q factor and f_r); A: Coil spacing [μm], B: Cu thickness [μm], C: Ferrite thickness [μm], D: Permeability.

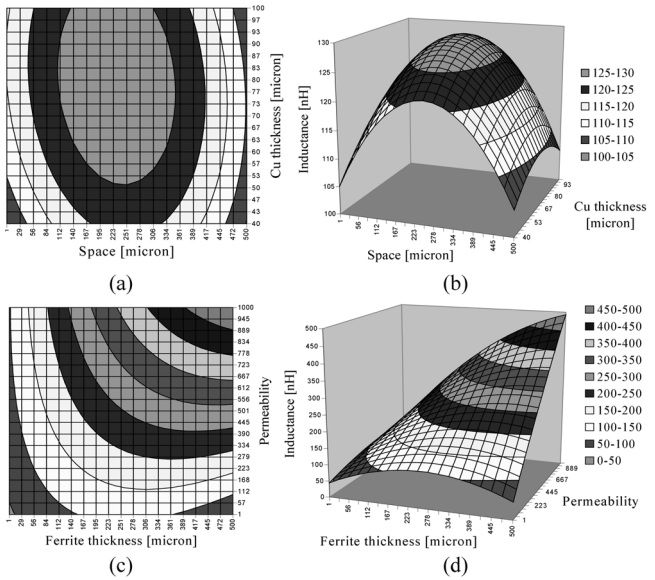

Fig. 5. Effects of 4 *X*'s on the inductance; (a), (b) coil spacing and Cu thickness at ferrite thickness of 130.3 μm and permeability of 156.5, (c), (d) ferrite thickness and permeability at coil spacing of 127.0 μm and Cu thickness of 67.8 μm.

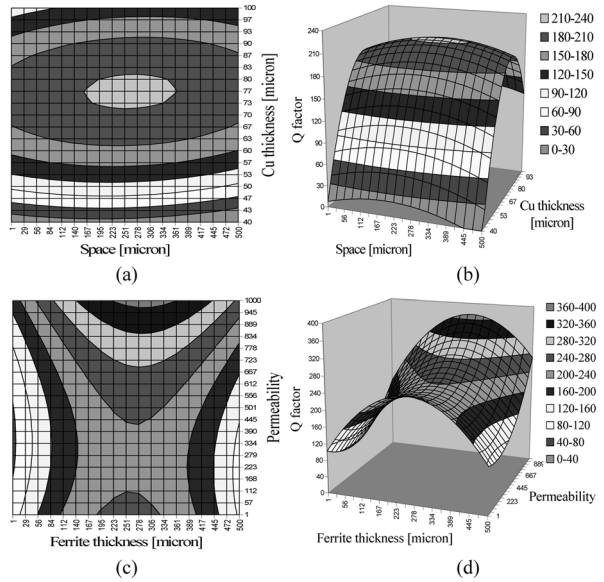

Fig. 6. Effects of 4 *X*'s on the Q factor; (a), (b) coil spacing and Cu thickness at ferrite thickness of 130.3 μm and permeability of 156.5, (c), (d) ferrite thickness and permeability at coil spacing of 127.0 μm and Cu thickness of 67.8 μm.

mension on the L seemed insignificant. In principle, L is defined as $L = \Phi/i$ (Φ: magnetic flux, i: current). Φ is dependent on ferrite thickness and μ since coil turns and coil width are fixed parameters.

Q factor of the inductor is logarithmically increased with ferrite thickness increases in the 1~250 μm range. However, opposite relation is shown in the 250~500 μm range as displayed in Fig. 6(c) and (d). When ferrite thickness is thicker than coil spacing, each facial sides of the ferrite around the inner port of the inductor are getting closer. Correspondingly, as the surface of the ferrite side wall gets bigger, C_{22} will be increased. Consequently, Q will decrease when R increases. In fact, C_{22}s are 0.754 and 10.1 pF when ferrite thicknesses are 251 and 500 μm, respectively, when parameters are the same with coil spacing of 251 μm, coil thickness of 75 μm, permeability of 501, in both inductors.

The percent difference in C_{22} is almost 172%. As for Cu thickness, Q factor increases up to 77 μm; oppositely, it decreases when Cu is thicker than 77 μm. This tendency comes from the skin depth effect. The Cu thickness should be 3.67 times the skin depth, but this is thicker than the predicted reasonable Cu thickness of 42 μm (= a thickness double the skin depth at 10 MHz).

The f_r of inductor can be defined as $f_r = 1/2\pi(LC)^{0.5}$. The coil spacing is the most influential factor on the f_r, because it can affect the L and C. The next influential factors are μ and ferrite thickness, which also influence L.

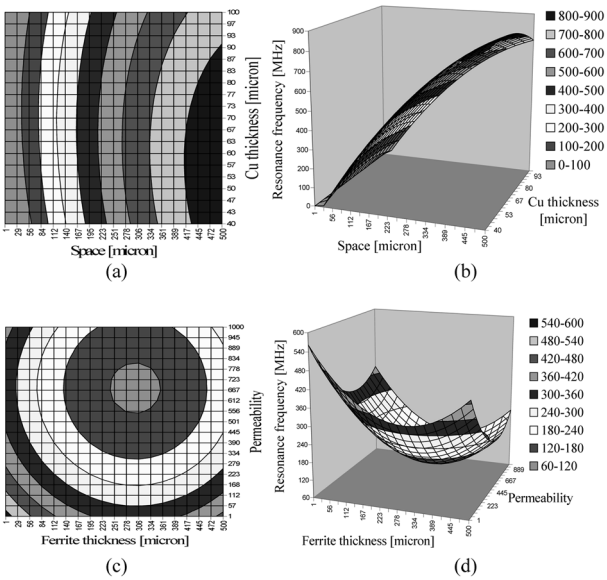

Fig. 7. Effects of 4 *X*'s on the resonance frequency; (a), (b) coil spacing and Cu thickness at ferrite thickness of 130.3 μm and permeability of 156.5, (c), (d) ferrite thickness and permeability at coil spacing of 127.0 μm and Cu thickness of 67.8 μm.

Each regression equation on the three Ys is derived and shown in Table 2. The R^2 of each equation, sample coefficient of determination (= SST – SSE = SSR/SST; SSR: sum of squares regression, SSE: sum of squares error, SST: sum of squares total), are 0.9854, 0.7175, and 0.9687 by computation for L and Q at 10 MHz and f_r, respective-

Table 2. Derived Regression Equations.

	Uncoded Regression Equation	R^2
L at 10 MHz [nH]	= 13.293 + 0.09878A + 0.65555B + 0.53978C + 0.11109D – 0.0000426AB – 0.0000812AC + 0.0000558AD – 0.0001863BC – 0.0002656BD – 0.0001676CD + 0.0000008ABC + 0.0000005ABD + 0.0000023ACD + 0.0000121BCD – 0.0002668A2 – 0.00487B2 – 0.00101C2 – 0.0000524D2	0.9854
Q factor at 10 MHz	= –733.47 + 0.11895A + 21.957B + 1.216C – 0.17608D + 0.0005252AB – 0.0000352AC + 0.0000288AD – 0.0004287BC – 0.000311BD – 0.0000449CD – 0.0000008ABC + 0.0000018ABD – 0.0000017ACD + 0.0000027BCD – 0.0003453A2 – 0.14519B2 – 0.0023C2 + 0.0002533D2	0.7175
f_r [MHz]	= –66.78 + 3.198A + 7.774B – 1.259C – 0.50797D – 0.00173AC – 0.00151AD + 0.0004264BD + 0.0000022ABC + 0.0000042ABD – 0.0000017BCD – 0.00214A2 – 0.06075B2 + 0.00252C2 + 0.0004861D2	0.9687

ly. In the case of the Q factor, R^2 is lower than the other cases, because Q is computed from equation (9), therefore, fluctuation by both errors on L of equation (7) and R of equation (8) participate together. The optimized values of the 4 *Xs* were calculated by multiple response optimizations with the regression equations. The inductor performances of *Ys* with optimum input design parameters, *Xs*, are summarized in Table 3. Inductance of 125 nH, Q factor of 197.5, and f_r of 316.3 MHz were calculated at coil spacing of 127 μm, Cu thickness of 67.8 μm, ferrite thickness of 130.3 μm, and permeability 156.5. However, no magnetic loss ($tan\ \delta = 0$) is assumed in all the evaluations. Q will be decreased to 50% at loss $tan\ \delta = 0.01$ and to 70% at 0.02. Thus, Q factor of about 60 is achievable with loss $tan\ \delta$ of 0.02. In addition, we optimized the 3 *Xs* when thickness of ferrite film was fixed at 3 μm for consideration of difficulties on the over 100 μm thick ferrite film processes. According to the result, inductance of 66.1 nH, Q factor of 74.6, and f_r of 632.4 MHz are expected at coil spacing of 210 μm, Cu thickness of 64 μm, ferrite thickness of 3 μm, and permeability 200. These calculated results by regression equations and simulated results by 3D remodeling with optimized *Xs* are compared to confirm the deviations of the equations. Differences of both results are –9.1% in L, 2.8% in Q factor, and 4.1% in f_r.

Table 3. Inductor performances of Ys for optimized Xs.

	L [nH]	Q factor	Fr [MHz]
Coil spacing of 127 μm, Cu thickness of 67.8 μm, ferrite thickness of 130.3 μm, and permeability 156.5	125	197.5	316.3
Coil spacing of 210 μm, Cu thickness of 64 μm, ferrite thickness of 3 μm, and permeability 200	66.1	74.6	632.4

4. Conclusion

Optimized design parameters for a high Q, high current ferrite inductor for 10 MHz switching, 1~2 W on-chip power module for the baseband chip of smart phone were proposed and demonstrated. In this work, three regression equations on the *Ys* were derived by DOE. Four *Xs* were optimized using these equations. From results, we have successfully designed a 5×5 mm^2 ferrite inductor which has Q above 50 at 10 MHz. The following design parameters, 2.5 turns of coil, coil line width of 500 μm, Cu coil thickness of 64 μm, loss $tan\ \delta < 0.02$, ferrite thickness > 3 μm, and permeability > 157 were determined to achieve an inductor with Q factor over 50 at 10 MHz. In addition, it was found that the optimized value of coil spacing is dependent on the ferrite thickness. Therefore, recalculations by regression equations are recommended for another ferrite thickness.

Acknowledgement

This work was supported by Air Force Research Laboratory under Grant FA 9453-06-I-0355.

References

[1] S. C. O. Matuna, T. O'Donnell, N. Wang, and K. Rinne, "Magnetics on Silicon: An Enabling Technology for Power Supply on Chip", IEEE Trans. on Power Electronics, **20** (3), 585 (2005).

[2] Enpirion, Inc. (2007). *Products information of Enpirion, Inc.* Available: http://www.enpirion.com/Productdetails.aspx?pid=7

[3] P. Hazucha, S.-T. Moon, G. Schrom, F. Paillet, D. S. Gardner, S. Rajapandian, and T. Karnik, "High Voltage Tolerant Linear Regulator With Fast Digital Control for Biasing of Integrated DC-DC Converters", IEEE J. of Solid-State Circuits, **42**, 66 (2007).

[4] P. Hazucha, G. Schrom, J.-H. Hahn, B. A. Bloechel, P. Hack, G. E. Dermer, S. Narendra, D. S. Gardner, T. Karnik, V. De, and S. Borkar, "A 233-MHz 80%-87% efficient four-phase DC-DC converter utilizing air-core inductors on package", IEEE J. of Solid-State Circuits, **40**, 838 (2005).

[5] G. Schrom, P. Hazucha, F. Paillet, D. J. Rennie, S-T

Moon, D. Gardner, T. Kamik, P. Sun, T. T. Nguyen, M. J. Hill, and K. Radhakrishnan, Memioglu, "A 100 MHz Eight-Phase Buck Converter Delivering 12A in 25 mm^2 Using Air-Core Inductors", IEEE 21th APEC, 727 (2007).

[6] S. Bae, Y. K. Hong, J. J. Lee, J. Jalli, G. S. Abo, A. Lyle, H. Han, and G. W. Donohoe, "High Q Ni-Zn-Cu ferrite inductor for on-chip power module", submitted to IEEE Transactions on Magnetics, May 2008.

[7] I. Kowase, T. Sato, K. Yamasawa, and Y. Miura, "A planar inductor using Mn-Zn ferrite/polyimide composite thick film for low-voltage and large-current DC-DC converter", IEEE Trans. on Mag., **41**, 3991 (2005).

[8] S. Prabhakaran, C. R. Sullivan, T. O'Donnell, M. Brunet, and S. Roy, "Microfabricated coupled inductors for DC-DC converters for microprocessor power delivery", 35th IEEE Power Electronics Specialists Conf., **6**, 4467 (2004).

[9] P.-L. Wong, F. C. Lee, P. Xu, and K. Yao, "Critical inductance in voltage regulator modules", IEEE Trans. on Power Elec., **17**, 485 (2002).

[10] T. Nakamura, "Snoek's limit in high-frequency permeability of polycrystalline Ni–Zn, Mg–Zn, and Ni–Zn–Cu spinel ferrites" J. of Appl. Phys., **88**, 348 (2000).

[11] M. Nakano, M. Akase, H. Fukunaga, Y. Matsuo, S. Yabukami, M. Yamaguchi, and K. I. Arai, "Permeability in PLD-made Mn-Zn ferrite thin films by low-temperature process", J. of Magn. and Mag. Mater., MM, **242-245**, 157 (2002).

[12] Z. Qian, G. Wang, J. M. Sivertsen, and J. H. Judy, "Ni-Zn ferrite thin films prepared by facing target sputtering", IEEE Trans. on Mag., **33**, 3748 (1997).

[13] T. Kagotani, R. Kobayashi, S. Sugimoto, K. Inomata, K. Okayama, and J. Akedo, "Magnetic properties and microwave characteristics of NiZnCu ferrite film fabricated by aerosol deposition method", J. of Magn. and Mag. Mater., **290-291**, 1442 (2005).

[14] N. Matsushita, M. Tada, M. Shigemori, and M. Abe, "High deposition rate obtained for spin-sprayed Ni-Zn ferrite films without using ammonia ions", IEEE Trans. on Mag., **40**, 2817 (2004).

[15] S. Hashi, N. Takada, K. Nishimura, O. Sakurada, S. Yanase, Y. Okazaki, and M. Inoue, "Fabrication technique for over 10-μm-thick ferrite particulate film at room temperature", IEEE Trans. on Mag., **41**, 3487 (2005).

[16] T. Kuribara, M. Yamaguchi, and K-I. Arai, "Equivalent circuit analysis of an RF integrated ferromagnetic inductor", IEEE Trans. on Mag., **38**, 3159 (2002).